



**HAL**  
open science

# Perspectives and Current Trends on Hybrid Nanocomposite Materials for Photocatalytic Applications

Emerson Coy, Igor Iatsunskyi, Mikhael Bechelany

► **To cite this version:**

Emerson Coy, Igor Iatsunskyi, Mikhael Bechelany. Perspectives and Current Trends on Hybrid Nanocomposite Materials for Photocatalytic Applications. Solar RRL, 2023, 7 (7), 10.1002/solr.202201069 . hal-04059790

**HAL Id: hal-04059790**

<https://hal.umontpellier.fr/hal-04059790v1>

Submitted on 4 Oct 2023

**HAL** is a multi-disciplinary open access archive for the deposit and dissemination of scientific research documents, whether they are published or not. The documents may come from teaching and research institutions in France or abroad, or from public or private research centers.

L'archive ouverte pluridisciplinaire **HAL**, est destinée au dépôt et à la diffusion de documents scientifiques de niveau recherche, publiés ou non, émanant des établissements d'enseignement et de recherche français ou étrangers, des laboratoires publics ou privés.

# Perspectives and Current Trends on Hybrid Nanocomposite Materials for Photocatalytic Applications

Emerson Coy, Igor Iatsunskyi, and Mikhael Bechelany\*

Photocatalysis can be understood as the acceleration of chemical reactions by incident light. These reactions typically perform poorly without photoactivation and the presence of catalysts. Photocatalysis could find applications in a wide range of fields, such as renewable energy and environmental remediation. The advance in the photocatalysis field is driven by the development of innovative materials allowing a broad range of absorption and efficient charge separation. The most developed photocatalysts are inorganic semiconductors. An alternative approach to increase the efficiency of these photocatalysts is the design of organic–inorganic hybrid materials. Two classes of hybrid materials are largely investigated: 1) small molecules and 2) organic macromolecules or polymers. The polymers can have protective roles as well as photocatalytic and conductive properties. The last type of material is known as conductive polymer. Different types of conductive polymers have been investigated in the literature. This perspective will focus on the new trend in this field by first describing the use of machine learning in designing and understanding polymeric hybrid systems toward catalytic applications, followed by the description of four types of the most used organic–inorganic hybrid materials as photocatalysts based on chitosan, polydopamine, polyaniline and covalent organic frameworks.

photoactivation. Photocatalysis could find applications in a wide range of fields such as renewable energy (water splitting, CO<sub>2</sub> reduction, solar fuel production) and environmental (water treatment by removing pharmaceutical and pesticides contaminant, for instance, and improving air quality by reducing volatile organic compounds [VOCs]).<sup>[1]</sup>

The advance in the photocatalysis field is driven by developing novel, innovative materials that mainly allow light absorption and efficient charge separation.<sup>[2]</sup> The most developed photocatalysts are inorganic semiconductors such as metal oxides (such as ZnO, TiO<sub>2</sub>, WO<sub>3</sub>, SnO<sub>2</sub>, and CuO)<sup>[3,4]</sup> and chalcogenides (ZnS, CuS, CdS, Sb<sub>2</sub>S<sub>3</sub>, Cu<sub>2</sub>SnS<sub>3</sub>, and Cu<sub>2</sub>SnSe<sub>3</sub>).<sup>[5,6]</sup> In order to enhance the performance of these semiconductor catalysts, different strategies were investigated to reduce the recombination of photogenerated electron–hole pairs and to extend the absorption edge of these catalysts to the visible region of sunlight: 1) tuning of the morphologies, 2) doping to tune

the bandgap, 3) junction between several semiconductor materials,<sup>[7,8]</sup> and 4) combining with metallic and plasmonic nanomaterials (Cu, Pt, Au, Pd).<sup>[9,10]</sup>

An alternative approach to increase the efficiency of these photocatalysts is the design of organic–inorganic hybrid materials. Two classes of hybrid materials were largely investigated: 1) small molecules such as dyes and molecular catalysts known for their sensitizing and photocatalytic properties, and 2) organic macromolecules or polymers are known for tuning the properties of the semiconductor. These polymers also act as a protective layer, tuning the composites' hydrophobicity/hydrophilicity or lipophilicity. Moreover, they could also provide additional photocatalytic, electron transferring, and conductive properties.

Different types of polymers were investigated in the literature, such as polydopamine (PDA), polyaniline (PANI), polythiophene, poly(3-hexylthiophene) (P3HT), polyphenylenevinylenes (PPVs), poly(3,4-ethylenedioxythiophene) (PEDOT), chitosan (CS), poly(pyrrole) (PPy), polyvinyl alcohol (PVA), covalent organic polymer (COP), and covalent organic frameworks (COFs).<sup>[11]</sup>

Two of the most well-established aforementioned conductive polymers are CS and PANI. Despite more than a century of ongoing research, these polymers continue to have a large and high-impact on the literature, as shown by the constantly growing research works published each year. This ever-increasing attention is primarily attributed to the extensive application of both

## 1. Introduction

Photocatalysis can be understood as the acceleration of chemical reactions by incident light, especially when the catalyst is photoactive. These reactions are unachievable or very difficult without

E. Coy, I. Iatsunskyi  
NanoBioMedical Centre  
Adam Mickiewicz University  
61-614 Poznan, Poland

M. Bechelany  
Institut Européen des Membranes  
IEM  
UMR 5635  
CNRS  
ENSCM  
University of Montpellier  
34730 Montpellier, France  
E-mail: mikhael.bechelany@umontpellier.fr

 The ORCID identification number(s) for the author(s) of this article can be found under <https://doi.org/10.1002/solr.202201069>.

© 2023 The Authors. Solar RRL published by Wiley-VCH GmbH. This is an open access article under the terms of the Creative Commons Attribution License, which permits use, distribution and reproduction in any medium, provided the original work is properly cited.

DOI: 10.1002/solr.202201069

polymers in remediation and energy-related fields.<sup>[12]</sup> Additionally, PDA is a conductive biomimetic polymer with recently discovered photocatalysis applications. The rich chemistry of PDA and its analogues combined with its unconventional properties with semiconductor materials make it a material that will most definitely provide groundbreaking performance and modalities in the near future.<sup>[13]</sup> Finally, COFs have a timeframe of development and research as PDA. They are coordinated polymer networks with large porosity and robust stability, which have large applicability in energy storage<sup>[14]</sup> and purification.<sup>[15]</sup> Although several drawbacks have been found,<sup>[16]</sup> such as low electron transfer and reaction speed, their application in photocatalysis is actively researched.<sup>[17]</sup> As shown later in this article, recent publications have shown the rapid development in this field, making them strong candidates for the new generation of photocatalysts.

This perspective will focus on the new trend in this field by reporting first the use of machine learning (ML) in designing and understanding polymeric hybrid systems toward catalytic and photocatalytic applications following describing of four types of organic–inorganic hybrid materials used as photocatalysts and based on CS, PDA, PANI, and COFs.

### 1.1. Emerging Methods—ML

ML is undoubtedly one of the most important methods that have taken materials sciences by storm. ML is a powerful tool that aids in the designing and application of materials. ML relies on two essential aspects: the large availability of training datasets and the fast development of powerful computing tools widely available for researchers. These aspects have been steadily growing in the materials community in the last decade, owing it to its current success. Moreover, ML has shown unmatched results in classification, regression, clustering, probability estimation, or dimensionality reduction tasks, especially in high-dimensional data, like interatomic potentials and materials discovery.<sup>[18–20]</sup> However, ML requires a significant effort in the classification and correlation of data. Redundancy and noise are difficult to address, especially when predicting or analyzing new materials aiming for multiproperty design.<sup>[21]</sup>

In polymer sciences, it has mainly been applied in the study of perovskites and organic solar cells,<sup>[22–25]</sup> in the designing of microporous polymers,<sup>[26]</sup> high thermal conductivity,<sup>[27]</sup> and, more importantly for this work, light-driven heterogeneous catalysis.<sup>[28]</sup> Despite the attractiveness of this approach, not many works are entirely devoted to polymeric catalysts or photocatalytic hybrid systems. Here, we will present some of the latest works on the topic, which address the designing and understanding of polymeric hybrid systems toward catalytic and photocatalytic applications.

Several works have provided deeper insights into conductive polymers toward remediation and photocatalysis. Chun Lu et al. used ML models to predict the removal capability of CS toward heavy metals.<sup>[29]</sup> The authors evaluated flocculant characteristics, flocculation conditions (especially its pH), and heavy metal properties ( $\text{Cu}^{2+}$ ,  $\text{Pb}^{2+}$ ,  $\text{Cd}^{2+}$ ,  $\text{Zn}^{2+}$ ,  $\text{Ni}^{2+}$ ), also average molecular weight, the functionalization degree, and the presence of the amino, carboxyl, and mercapto groups, including their point zero

charge. The results showed that flocculation pH above 7.0, a concentration of 50–150  $\text{mg L}^{-1}$ , plus the molecular weight of the flocculant and its point zero charge below 7 pH provided better performance and removal (Figure 1a). Recently, T. Zhan et al. have shown a prediction of photocatalytic performance of lignin cleavage of C–C bonds.<sup>[30]</sup> Their model included the cleavage dissociation energy, the molecular dipole moment as input variables, and a DFT model. Their study shows that, as expected, the bandgap of the catalyst was the most important catalyst feature, followed by specific surface area, especially interesting was the negative influence of the methoxy groups, which provide higher stability to lignin, but reduced its dislocation efficiency (Figure 1b).

Despite the large applicability of ML, several issues must be solved. Many of the main aspects are already well known for a few years, much work is needed, and large databases are still missing.<sup>[21]</sup> Recently, Yuzhi Xu et al. have demonstrated how the use types of multidimensional fragmentation descriptors (MDFD), structure-based MDFD (SMDFD) and electronic property-based MDFD (EPMDFD), provided a much more efficient and accurate predictive model than traditional ML models.<sup>[31]</sup> As reported, the model was applied to copolymer assemblies to predict efficient polymeric-based hydrogen photocatalysts. As described by the authors, the method uses the idea of “divide-and-conquer,” and as a result, it was found that the delocalization of the excited state electrons in the A–B conjugated copolymers was of critical importance for the photocatalytic hydrogen evolution reaction (HER) process (Figure 1c).

In the future decade, ML is bound to play a significant role in the materials science community, especially because the evergrowing materials community continues to produce more complex hybrid systems with outstanding properties. Such results will not only provide larger datasets for ML analysis but will also demand the implementation of a more rational design for future photocatalysts.

### 1.2. Emerging Methods—Spatially Resolved Surface Photovoltage

The spatially resolved surface photovoltage (SRSPV) is a relatively new method for exploring charge distribution on photocatalytic materials at the micro- and nanoscale. The method has evolved from the already well-established Kelvin probe atomic force microscopy (K-AFM)<sup>[32]</sup> and includes the detection of photogenerated currents. SRSPV essentially measures the surface potential of semiconductor materials while exposed to light and, because of the superior spatial resolution of the AFM technique (nm), provides a unique spatial distribution of charges. The method has been used to map charge distribution on single-crystalline materials. Zhu et al. studied a  $\text{BiVO}_4$  single particle/crystal and showed a highly anisotropic charge distribution on the particle, with a variation of charge 70 times higher for [011] facets than [010].<sup>[33]</sup> The large anisotropy was attributed to the built-in electric field and played a role in the oxidation of molecules. The results advocate for facet engineering of photocatalysts, which is considered an important aspect of rational design in catalysts nowadays.<sup>[34]</sup> Gao et al. used the method to probe the phase charge separation between  $\text{TiO}_2$  anatase/rutile. They found an electric field of  $1 \text{ kV cm}^{-1}$  at the phase boundary. Upon illumination with UV, they showed a size-dependent

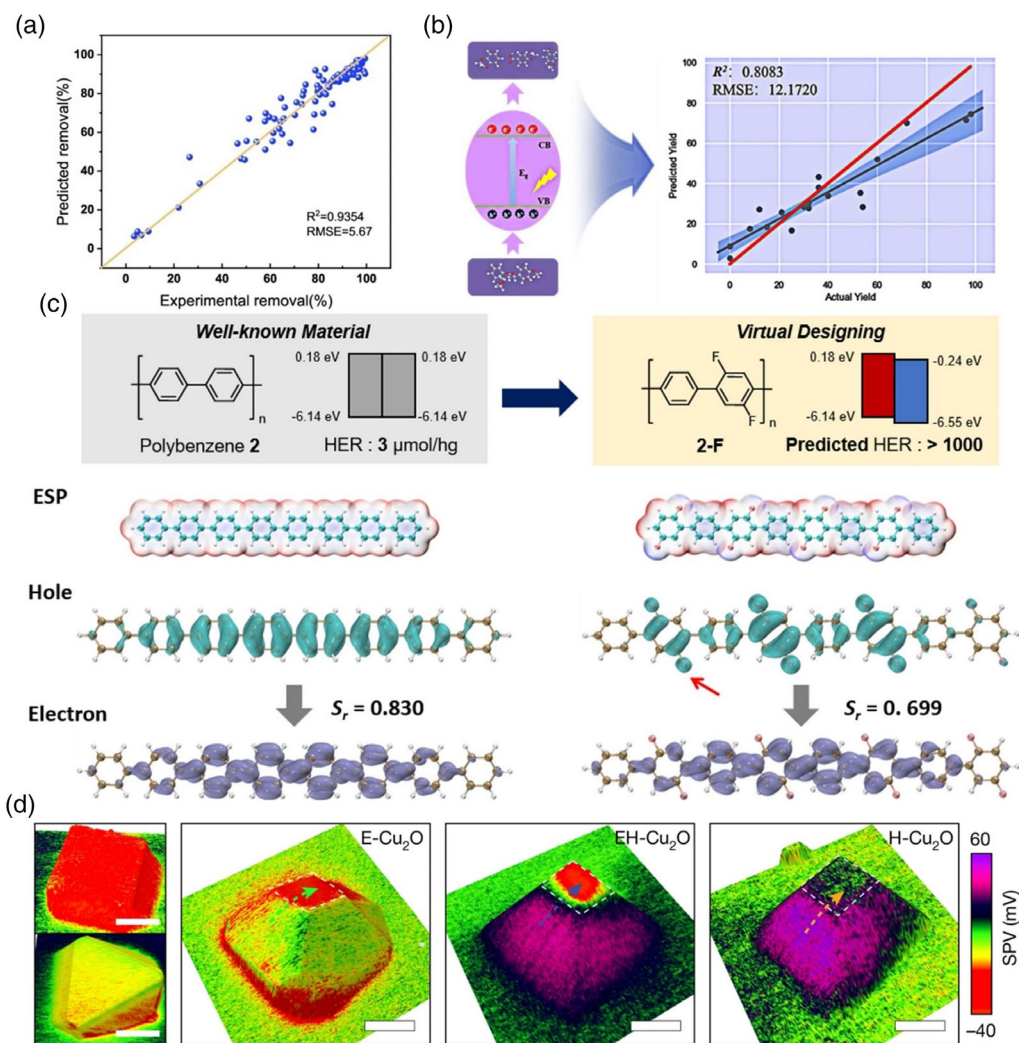


**Figure 1.** a) Scatter plot of the predicted heavy metals removal efficiency and experimental data using RF model. Reproduced with permission.<sup>[29]</sup> Copyright 2022, Elsevier. b) RMSE and  $R^2$  scores of products molecular yield predicted by RF regression model collecting data of photocatalytic lignin degradation breaking C–C bond as features. Reproduced with permission.<sup>[30]</sup> Copyright 2022, Elsevier. c) Electronic static potential, e-h distributions of *p*-polyphenyl 2 (left) and fluorine-substituted *p*-polyphenyl 2-F (right) with LC- $\omega$ PBE/6-31G\* ( $\omega$ -tuned); green and purple represent the hole and electron distribution, respectively. Reproduced with permission.<sup>[31]</sup> Copyright 2021, American Chemical Society. d) SPV images of Cu<sub>2</sub>O (left) cubic(001) and octahedral(111) particles. The other panels shown particles facet engineered to show mainly electrons (E-Cu<sub>2</sub>O), electron–holes (EH-Cu<sub>2</sub>O), and holes (H-Cu<sub>2</sub>O). Scale bars are 2  $\mu$ m. Reproduced with permission.<sup>[36]</sup> Copyright 2022, Springer Nature.

charge separation and an electron transfer from rutile to anatase.<sup>[35]</sup> This study is also important, as it showed the application of the method on polycrystalline phases as a model. Recently, Chen et al. have studied the spatiotemporally tracking of charge transfer in CuO<sub>2</sub> microcrystals (Figure 1d). They showed how, by facet engineering the surfaces to show both holes and electrons, the hydrogen production of CuO<sub>2</sub> microparticles was improved by the quasiballistic interfacet electron transfer.

Although the technique has reached a certain level of maturity, and a few reviews on the topic have fomented a steady increase study of multiple materials,<sup>[36–40]</sup> not much can be found for hybrid nanocomposites. Aubriet et al. have recently explored heterojunctions of PTB7-PC<sub>71</sub>BM (PTB7: poly[4,8-bis[(2-ethylhexyl)oxy]benzo[1,2-b:4,5-b']dithiophene-2,6-diyl][3-fluoro-2-[(2-ethylhexyl)carbonyl]thieno[3,4-b]thiophenediyl] and PC<sub>71</sub>BM:

[6,6]-Phenyl C71 butyric acid methyl ester), in tandem with Al<sub>2</sub>O<sub>3</sub> surfaces.<sup>[41]</sup> Their study used a slightly modified experimental system to include a time domain (pump-probe). As a result, they found rapid light-induced charge distribution on the surface, which otherwise would not be detectable in conventional experiments. The main advantage of these findings relies on the possible accurate identification of topographic recombination centers and perhaps the examination of faster effects.

Despite the limited literature on hybrid interfaces toward photocatalysis, it can be expected that studies on polymeric/semiconducting systems using SRSPV will be more prominent in the following years. This will, undoubtedly, provide essential insights into the electron-transferring mechanism governing these systems and, more importantly, an extra level in their control toward highly efficient catalysts.

## 2. Recent Advancements in CS-Based Nanocomposites

Among the many polymers that can be used to develop hybrid nanocomposites for photocatalysis, CS is considered one of the most promising and the one that presents more significant perspectives in applicability. CS is a natural carbohydrate biopolymer derived by *N*-deacetylation of Chitin (a linear polymer of *N*-acetyl-2-amino-2-deoxy-D-glucopyranose units with  $\beta$ -(1-4) bonds). CS is a biopolymer with cationic nature and one of the significant natural polysaccharides. It has various applications in environmental engineering,<sup>[42]</sup> biomedicine,<sup>[43]</sup> and photocatalysis.<sup>[44]</sup> Photocatalysts composed of semiconductors and CS, being biocompatible and eco-friendly, could be a practical approach in many applications.

Over the last 10 years, various nanocomposites based on semiconductor-CS have been developed. It was shown that TiO<sub>2</sub>-CS materials, by incorporating CS onto the TiO<sub>2</sub> surface, enabled the adsorption of both acid and basic dyes.<sup>[45]</sup> It was suggested that the amino groups of CS can be protonated. Consequently, the polymer can be expected to contribute to the charged interaction with anionic dyes. Besides, it can decrease the adsorption capacity of the semiconductor material for basic dye adsorption.

The modification of ZnO nanostructures by CS improved its photocatalytic efficiency as well. It was shown that the high adsorption capacity of ZnO-CS nanocomposites is due to the strong electrostatic interaction between the NH<sub>3</sub><sup>+</sup> of CS (amino group (-NH<sub>2</sub>)) was easily protonated to form -NH<sub>3</sub>.<sup>[46,47]</sup>

Another example is CdS-CS nanocomposites. Zhu et al. synthesized the cross-linked CS/CdS nanocomposite prepared by simulating the biomineralization process.<sup>[48]</sup> The protonation of CS amino groups has again explained the photocatalytic efficiency of advanced nanocomposites at a low pH. The authors demonstrated that the CS layer improves the absorbance of dye anions because of electrostatic attraction.<sup>[48]</sup>

Recent research demonstrates the capability of CS to enhance photocatalytic activity not only in metal oxide semiconductors but also in selenides, sulfides, and nitrides. Shen et al. developed the carbon-doped g-C<sub>3</sub>N<sub>4</sub> and CS nanocomposites for pathogenic biofilm control.<sup>[49]</sup> They demonstrated that the developed nanocomposites possess a high photocatalytic activity that continuously generates reactive oxygen species (ROS) and hence inactivates pathogens. This research uses CS as a self-cleaning matrix for immobilizing the photocatalysts—carbon-doped g-C<sub>3</sub>N<sub>4</sub>. The g-C<sub>3</sub>N<sub>4</sub> particles were uniformly distributed in the CS matrix, which is crucial for effective photocatalysis and biofilm inhibition.<sup>[49]</sup> In other research, the ZnSe nanoparticles were incorporated into the CS matrix to enhance their activity and avoid leaching.<sup>[50]</sup> The developed ZnSe-CS nanocomposites showed excellent photocatalytic degradation efficiency for tartrazine and other organic dyes.

Sirajudheen et al. demonstrated that the presence of reactive hydroxyl (-OH) and amino (-NH<sub>2</sub>) groups on the surface of CS enables the adsorption ability toward organic and inorganic pollutants, making it a highly promising material for decontamination purposes. However, some drawbacks of CS, including low porosity and the sensitivity to pH changes, may limit its

application.<sup>[51]</sup> One of the possible solutions to surpass those CS drawbacks is to combine it with other polymers that are more resistant to acidic environment. They demonstrated that the CS-PANI/ZnS composite could efficiently affect dye removal via simultaneous adsorption and photodegradation mechanism with excellent reusability in different pH.

Janani's group applied a similar approach. They synthesized by coprecipitation, and ultrasonic-assisted method novel photocatalysts based on CuO-loaded ZnS nanoflower supported on carbon framework PVA (polyvinyl alcohol)/CS.<sup>[52]</sup> CS and PVA were also used as a supporter for metal sulfide and oxide nanoparticles. PVA was chosen for its excellent chemical and physical resistance properties. The developed multifunctional ZnS-CuO/PVA/CS nanocomposite was promising for the photocatalytic degradation of tetracycline and as an antimicrobial agent.

Another approach to overcome the drawback of CS is the synthesis of CS-based hydrogel. It is known that many hydrogels are capable of excellent photocatalytic performance. An alkaline CS-based hydrogel was recently prepared using a simple freezing-thawing process.<sup>[53]</sup> A similar methodology was applied to synthesize the alkaline CuO@CS-H photocatalysts with enhanced photocatalytic activity for biomass-derived sugars reforming to lactic acid and with increased stability of CuO nanoparticles.<sup>[54]</sup>

The last approach in applying CS-based composites could be related to the combination of CS with a new class of materials—COFs. The application of COF for photocatalysis will be shown in the next sections. However, we would like to underline the application of CS as a support of COFs. Recent research of Tong's group demonstrated that the novel nanocomposites based on CS (the film-substrate) and COFs could effectively degrade 99.8% of paracetamol (PCT) and 94.0% of bisphenol A (BPA) within 180 min under visible light irradiation (**Figure 2a**).<sup>[55]</sup> They proved that CS is an excellent substrate for the fabrication of COFs film.

We may draw the main features of the perspective usage of CS for photocatalytic applications. First of all, the protonation of the CS amino groups leads to a positive surface charging that may increase the efficiency of photocatalytic properties due to a higher concentration of adsorbed molecules. Second, CS may act as a matrix containing photocatalytic material evenly distributed over the polymer. The last, recent scientific trends indicate that CS may be employed as a substrate to support the synthesis of COF or metal-organic frameworks (MOF) (**Figure 2b**). We can also assume the possible prospects of using CS for photocatalysis. Perhaps one of the applications of CS will be its combination with 2D materials, e.g., MXenes. MXenes are 2D transition metal carbides and nitrides. MXenes have been widely used in energy,<sup>[56]</sup> sensors,<sup>[57]</sup> and (photo)catalysis<sup>[58]</sup> due to their superior properties, such as enhanced near-infrared (NIR) responsiveness, hydrophilicity, excellent mechanical strength, and surface chemistry. Recently, it was demonstrated the application of CS/MXene nanocomposites for photothermal therapy,<sup>[59]</sup> electromagnetic shielding<sup>[60]</sup> (**Figure 2b**), water purification,<sup>[61]</sup> and sensing.<sup>[62]</sup> However, there is still plenty of room for developing and applying CS/MXene nanocomposites in photocatalysis.

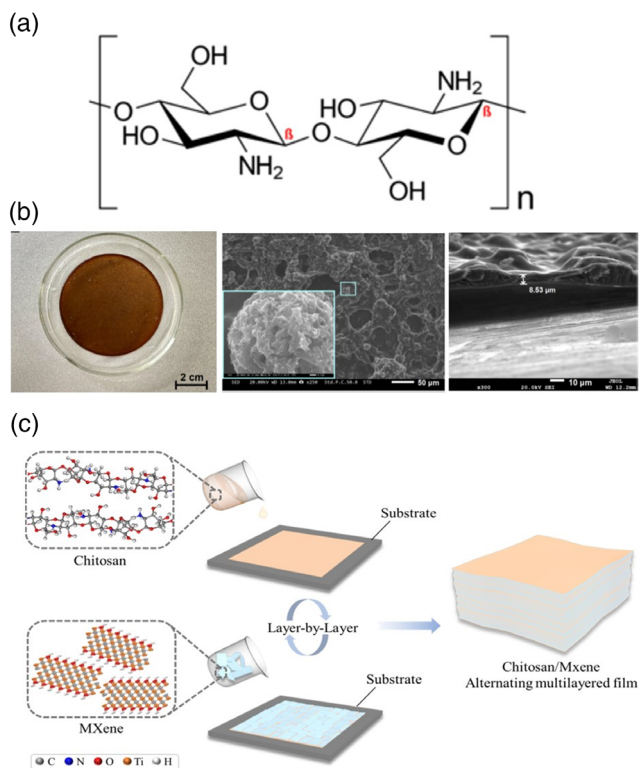


**Figure 2.** a) The CS molecule; b) the photo and SEM images of CS-COF nanocomposites. Reproduced with permission.<sup>[55]</sup> Copyright 2022, Elsevier. c) Schematic description of the fabrication process of CS/MXene multilayered film. Reproduced with permission.<sup>[60]</sup> Copyright 2022, Elsevier.

### 3. Recent Advancements in PDA Composites

PDA is a biomimetic polymer that has shaken the materials community due to its simple polymerization pathways, easy application on virtually every surface, and unique chemistry that allows it to be used as an initiator on many complex syntheses,<sup>[63,64]</sup> tandem structures,<sup>[65]</sup> or as a biocompatible component in many heterostructures.<sup>[66]</sup> PDA was originally synthesized in 2007 by Lee et al.,<sup>[67]</sup> as the result of the oxidation of dopamine. Although straightforward, PDA polymerization does not result in an easily characterisable polymer. Thus, it does not allow for comprehensive structural characterization or prescreening of the physical-chemical properties of PDA.<sup>[68]</sup> This impossibility is mainly due to the elusiveness of its structure, which remains a challenge nowadays.<sup>[69]</sup>

PDA materials are typically polymerized by different methods, mainly direct wet polymerization,<sup>[70]</sup> air-water interface,<sup>[71]</sup> and electrochemical methods.<sup>[72]</sup> They can be obtained as nanoparticles, porous nanoparticles,<sup>[73]</sup> films, and composites. Despite their large applicability and rather well-established application in many fields, such as photocatalysis<sup>[74]</sup> and sensors,<sup>[72]</sup> there is not much consensus on the physical properties of this material. Generally, the properties and molecular structure of PDA nanostructures vary between synthesis and, therefore, between research groups. Nevertheless, the commonly accepted structure of PDA contemplates a random (amorphous) distribution of polymeric units of 1, 2, 3, 4, and 5 units, organized consisting

of indole and dopamine units at various oxidation states,<sup>[66]</sup> with two main radicals in its structure.<sup>[75]</sup> Despite this, several studies have pointed to the inherent  $\pi - \pi$  stacking of the PDA structures and the possibility of having a semiordered supramolecular assembly of PDA.<sup>[73]</sup> To this day, only a few reports have shown this 2D-like organization,<sup>[76]</sup> which shows that this polymer remains highly relevant and challenging even at a basic level.

A generalization of the properties of PDA is often difficult, especially because several of its properties strongly depend on its hydration level. For instance, its electrical conductivity is reported to change from  $10^{-13}$  to  $10^{-5}$  S m<sup>-1</sup> from dry to fully hydrated.<sup>[74]</sup> The refractive index ( $n$ ) has also been reported to be somewhere between  $1.5 < n < 1.8$ .<sup>[74]</sup> Additionally, the mechanical properties of PDA have been tested both by contact and noncontact means, and the results show a sizeable elastic modulus of  $13 \pm 4$  GPa, a value rather large for thin film polymeric samples.<sup>[77]</sup> This ambiguity and lack of standardization on PDA base materials is a significant challenge that needs to be addressed by the community in the following years, especially when aiming for a general and interlaboratory “standard” for PDA materials. Also, although much research is devoted to reproducible synthetic conditions, the dispersion of physical properties poses an additional challenge for these materials.

One of the most interesting and fundamental aspects of PDA is its often overlooked behavior as an organic catalyst. Due to the catechol-quinone moieties, PDA shows an oxygen-mediated nonradical pathway via a quinone-imine step.<sup>[78]</sup> Mrówczyński et al. previously observed a related effect in PDA-coated magnetite composites, where PDA worked as an organocatalyst in direct aldol reaction.<sup>[79]</sup> Nevertheless, it has remained prevalent in nanoparticle research because it is known that it does not show any photocatalytic activity on its own. However, this is not the case when this polymer is used in combination with semiconductor materials, in which case it acts as a sensitizer for photocatalytic processes.<sup>[74]</sup>

#### 3.1. PDA/Semiconductor Interfaces

The combination of nanometer-thick PDA coatings with direct bandgap semiconductor materials has shown unexpected and fascinating results for photocatalytic applications. Although the enhancement effect of PDA on semiconductor nanoparticles has been known for some time,<sup>[74,80]</sup> recently, several studies have shown extraordinary results beyond the well-established TiO<sub>2</sub> and ZnO. Researchers have looked to the PDA coating of other complex materials, such as ZnS and CdS, which have shown outstanding enhancement toward photocatalytic hydrogen production.<sup>[74]</sup>

Although it has been shown that PDA reduces the optical bandgap of nanomaterials, by as much as 0.4 eV, the reason is still unknown. However, the effect has been previously reported in the literature.<sup>[74,81–83]</sup> In the case of metal oxides, PDA attaches by the covalent binding of oxygen to the surface. In this attachment, PDA compensates for oxygen vacancies on the surface and reduces recombination rates, boosting the optical and photocatalytic response.<sup>[84]</sup> Moreover, it was recently shown that PDA/ZnO compensates the surface defects and produces H<sub>2</sub>O<sub>2</sub> with a  $1011.4 \mu\text{mol L}^{-1} \text{h}^{-1}$ , which is almost 9 times higher than PDA

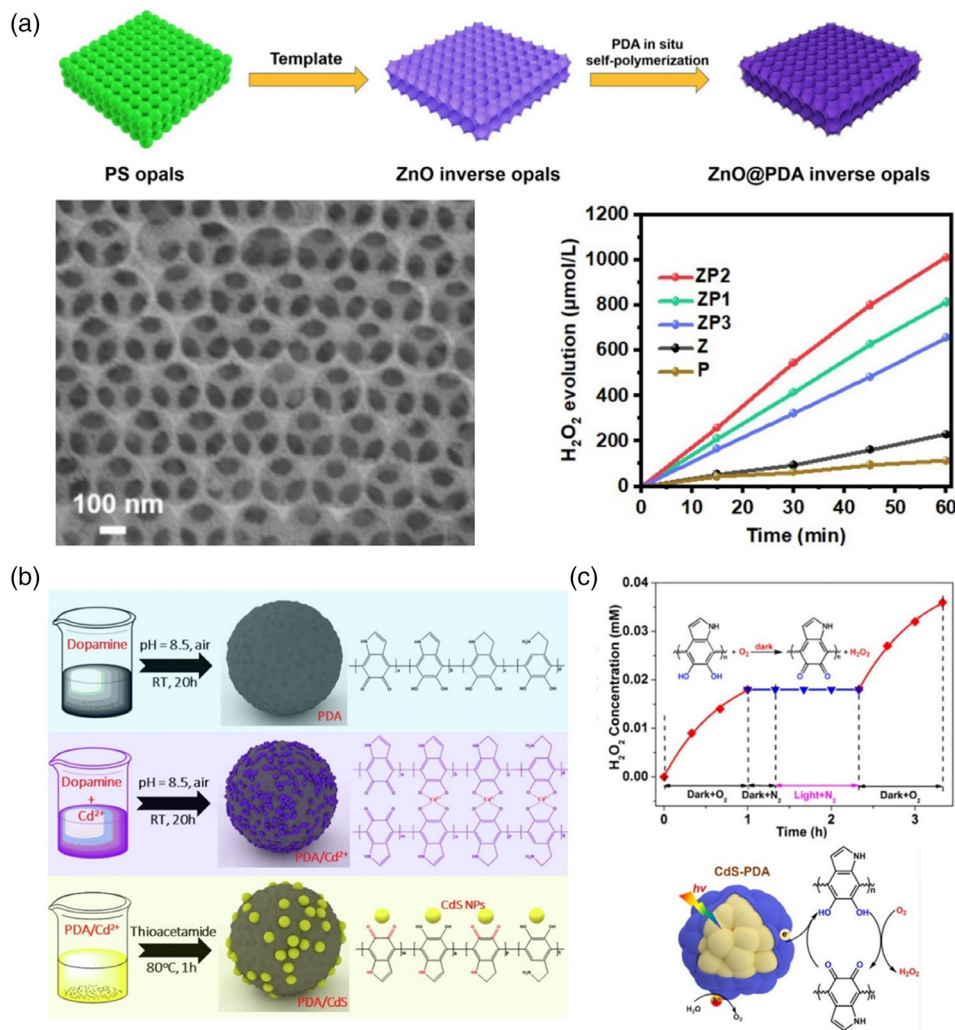


**Figure 3.** a) TiO<sub>2</sub>/PDA inverse opal catalyst elemental mapping (top). Photocatalytic production of H<sub>2</sub>O<sub>2</sub> for different TiO<sub>2</sub>/PDA weight loads (bottom, left). Schematic of the S-Scheme charge transfer mechanism, with labelled time scales for electron trapping, interfacial transfer, and recombination rates (bottom, right). Reproduced with permission.<sup>[87]</sup> Copyright 2022, American Chemical Society. b) Schemes illustrating the synthesis procedure of (top) PDA and (mid, bottom) PDA/CdS photocatalyst with dopamine hydrochloride, Cd(NO<sub>3</sub>)<sub>2</sub>, and thioacetamide. Reproduced with permission.<sup>[88]</sup> Copyright 2022, Elsevier. c) (Top) H<sub>2</sub>O<sub>2</sub> production on CdS–PDA under different control conditions. Reaction conditions: catalyst (100 mg), water (0.1 L), O<sub>2</sub>-saturated atmosphere in the dark or N<sub>2</sub>-saturated under Xe lamp ( $\lambda > 420$  nm). Mechanism of photocatalytic H<sub>2</sub>O<sub>2</sub> by the sustainable transformation of CdS–PDA (bottom). Reproduced with permission.<sup>[91]</sup> Copyright 2022, American Chemical Society.

and ZnO alone. This enhancement is attributed to an S-scheme heterojunction between PDA and ZnO.<sup>[85]</sup> Moreover, the effect has also been observed recently in C<sub>3</sub>N<sub>4</sub>/PDA by Zhang et al., with 4 times higher yields of H<sub>2</sub>O<sub>2</sub> production than bare C<sub>3</sub>N<sub>4</sub>.<sup>[86]</sup> Wang et al., studied a similar effect<sup>[87]</sup> and determined that an inorganic/organic S-scheme heterojunction, with ultra-fast electron transfer between TiO<sub>2</sub> and PDA, was responsible for the enhancement in H<sub>2</sub>O<sub>2</sub> production (Figure 3a).

Nevertheless, in other materials, such as sulfides, the covalent binding of PDA was expected to have a detrimental effect on the general performance of the nanocomposite. Similar to the case of FeS<sub>2</sub> (Pyrite), whose bandgap is lost due to surface effects, it was generally expected that PDA would ruin the applicability of such materials. However, Kim et al. showed in the case of ZnS, the covalent binding of PDA over the surface of ZnS nanowires

generated a passivating ZnS<sub>1-x</sub>O<sub>x</sub> layer that avoided further oxidation and degradation of the nanowires during photocatalytic processes. Moreover, it was shown that similar to metal oxides, the bandgap of ZnS was reduced by 0.3 eV, and the photocatalytic efficiency was exceptionally high. The hydrogen evolution reaction showed a hydrogen production of 2162.5 μmol h<sup>-1</sup> g<sup>-1</sup> and a significant stability of 78.7% after 24 h without cocatalyst inclusion.<sup>[88]</sup> Recently, Wang et al. have used the chelating properties of PDA toward Ca<sup>2+</sup> to improve the photocatalytic behavior of PDA/CdS nanocomposites, without losing Cd ions. Their catalyst also performed exceptionally at ≈1066 μmol h<sup>-1</sup> g<sup>-1</sup> (Figure 3b).<sup>[89]</sup> Similarly, Liu et al. proposed a CdS@PDA@SnO<sub>2-x</sub> nanocatalyst to exploit the chelating properties of PDA and avoid S<sup>2-</sup> losses that lead to the oxidation of CdS. The authors reported an increase of hydrogen evolution

production of 34.3 times over that of pristine CdS.<sup>[90]</sup> This enhancement effect of PDA in sulfides was also observed by Lu et al. who synthesized CdS/PDA nanorods with an improved photocatalytic performance (14.2 times higher than traditional CdS) and larger light absorption in the visible spectra, showing that morphological strategies (nanoparticles, layer, and nano-wires) are also compatible with PDA.<sup>[91]</sup> Finally, Wei et al. have shown that similar to the ZnO/PDA case, CdS/PDA has enhanced and selective production of H<sub>2</sub>O<sub>2</sub>, with a yield of 3.84 mM in 24 h under visible light, a result that is 13.7 times higher than that of CdS (Figure 3c).<sup>[92]</sup>

### 3.2. PDA-Based Film

After the discovery of PDA, researchers explored several ways of obtaining novel materials and morphologies, nanoparticles, nanotubes, and thin films/coatings.<sup>[93]</sup> Several studies examined the films and their potential applications, with most of the attention being given to films obtained by direct polymerization<sup>[94]</sup> or electrochemical oxidation.<sup>[72]</sup> However, during the oxidation of dopamine, the air–water interface produces a visible film, which is often lost due to vigorous stirring. Quite recently, there has been a new interest in these films. This is because it has been shown that they are exceptionally hard with  $13 \pm 4$  GPa and, more importantly, exhibit an ordered supramolecular structure that was not seen before in PDA nanostructures.<sup>[76]</sup> The origin

of the structure is still unclear, but the limited chemical pathways in the reaction clearly suggest a PDA-related structure. Szweczyk et al. have examined the growth in detail and obtained largely scalable and easily transferable films. Additionally, with the help of molecular dynamic simulations, it has been theorized that the air–water surface works as a template playing a significant role in stacking PDA tetramers (Figure 4a).<sup>[95]</sup>

Electrochemically grown films have been studied in detail in the literature, with some important insights on the polymerization provided recently by Olejnik et al. in their study. They found that catechol units are more likely polymerized than quinone forms. Additionally, it was shown that electropolymerization occurs in a small range of voltages, 0.0 to +0.4 V, while the extended range, –0.5 to 1.0 V, is responsible for the PDA layer formation.<sup>[96]</sup> These findings opened the door for a further study on the preparation of copolymer between Zwitterion and dopamine (polydopamine). These films showed outstanding sensitivity, 5 times higher than bare boron-doped carbon nanowalls (BCNW), toward detecting neurotransmitters.<sup>[97]</sup> More importantly, their studies show the versatility of the electrochemical method overall. While the air–water interface can provide large area and scalability, the electrochemical oxidation provides chemical “control” over the oxidized species and allows for tailoring more complex composites. Furthermore, Nothling et al. showed how PDA works as an anchor point for the attachment of propagating vinyl polymer macroradicals through radical–radical coupling.<sup>[98]</sup> The process further

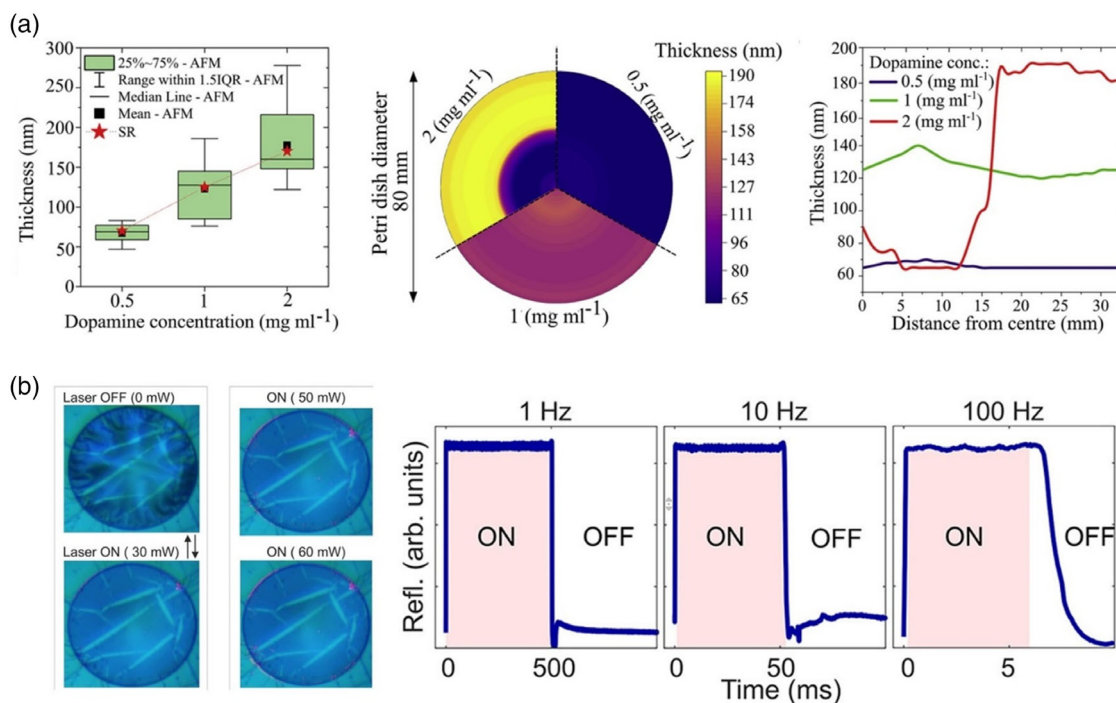


**Figure 4.** a) (Left) Box (AFM) and point (SR) comparative charts of film thicknesses for different dopamine concentrations. (Middle) Mapping of film thickness for different dopamine concentrations along film radius with a resolution of 1 mm by SR method. (Right) Line chart (SR) of film thickness for different dopamine concentrations along the radius of the film. Reproduced with permission.<sup>[95]</sup> Copyright 2022, Elsevier. b) (Left) Optical images of a PDA membrane subjected to light-induced contraction at ambient conditions. The power of the incident red laser light is 30 mW. The red laser light in the ON state is not visible due to the optical filter F. The photoactuated state (laser ON) of the PDA membrane at 50 and 60 mW laser power (upper and lower panels, respectively). (Right) Periodic contraction and flattening of an irradiated PDA membrane. The membrane becomes flat for 0.5 s, 50 ms, and 6 ms with a repetition rate of 1, 10, and 100 Hz, respectively. Reproduced with permission.<sup>[99]</sup> Copyright 2022, American Chemical Society.

enhances the rich chemistry of PDA and expands its potential for the functionalization of multiple surfaces.

Finally, an outstanding discovery was reported by Vasileiadis et al. where a light-driven mechanical contraction (photoactuation) was observed in PDA films.<sup>[99]</sup> In their report, a suspended thin film of PDA films (or membranes), grown by electrochemical methods, was excited by visible light. As a result, PDA films showed ultrafast contraction <140 μs, while expansion happens relatively slowly over millisecond time (Figure 4b). The results open a new branch of applications for PDA thin films, in actuation, sensing, and transduction.

#### 4. Recent Advancements in PANI Composites

PANI (PANI/PANi) is a relatively old conductive polymer discovered back in 1986, when it was known as aniline black. PANI currently exists in various forms depending on its oxidation levels. The fully oxidized PANI is known as pernigraniline base (blue/violet); half oxidized PANI as emeraldine base (green/blue), and fully reduced PANI as leucoemeraldine base (white/transparent).<sup>[100]</sup> From this group, emeraldine is the most conductive, with a conductivity reported around  $10^{-10}$  S cm<sup>-1</sup>. As in the case of many polymers, the actual conductivity depends on the preparation method. Besides its good electrical conductivity, PANI has excellent high-temperature resistance and environmental stability.<sup>[101]</sup> However, it also shows poor solubility in solvents, making it challenging to integrate into many architectures and its low processing capacity limits the applications in biomedicine. Additionally, PANI's superior stability means low biodegradability, which, depending on the application, might be considered a major drawback.<sup>[102,103]</sup> Furthermore, PANI electron transferring tends to require large protonation, which makes it a poor conductor at >5 pH. In many cases, these changes are irreversible.

PANI has intense coloration and conductive changes with oxidation state and doping, making it ideal for electrochromic architectures and sensing.<sup>[12]</sup> Among the fabrication methods available for PANI, electrospinning stands out as one of the most widespread, as it has been shown to prepare large areas of intricate fibers for different applications.<sup>[104]</sup> The main advantages that electrospinning provides over other methods are the lack of complex solvent, the easy integration of nanostructures and facile further functionalization, and integration in devices, with a broad range of fiber sizes, from millimetric to ultrafine micrometric ones,<sup>[105]</sup> making this process one of the most widespread and promising methods.

##### 4.1. PANI/Semiconductor

Recently, many composite-based applications have been reported using PANI matrixes for photocatalysis and water remediation.<sup>[106]</sup> Similar to other conductive polymers, the primary trend focuses on enhancing the electron transfer of photogenerated carriers by using the conductive polymer and protecting the catalyst from photocorrosion. Additionally, for example, Zhang et al. prepared SnS<sub>2</sub>/PANI composites by a combination of hydrothermal synthesis and direct polymerization. In this work, they prepared ternary samples of PANI/SnS<sub>2</sub>/NRG (nitrogen-doped

reduced graphene oxide) by a similar method.<sup>[107]</sup> The composite morphology showed SnS<sub>2</sub> nanoflakes 30–40 nm, surrounded by conformal granular PANI coating. The results showed an almost twofold efficiency and stability in the reduction of aqueous Cr(VI) by visible light (>420 nm). Although the mechanism is unclear, the composites showed improved electron transfer and reduction of resistance, as well as a slight bandgap reduction in the ternary composite. The authors performed a similar study on Zr<sup>4+</sup>-doped SnS<sub>2</sub> with PANI; the study showed further improvement associated with the larger absorption of the composite.<sup>[108]</sup>

Faisal et al. studied SrSnO<sub>3</sub> composites with PANI, toward the degradation of methyl blue using UV-vis.<sup>[109]</sup> The performance was 2 times faster than SrSnO<sub>3</sub> alone, with large recoverability. The increment in performance could be attributed to the bigger surface area of the composites versus the PANI content. Interestingly, the highest performance was observed for PANI 5% and a decrement in performance for the 10% sample. This suggests that there is an interplay between conductivity, surface and PANI content, or the thickness of polymer coating.

Studies focusing on TiO<sub>2</sub> composites are more plentiful, and it has become a relatively mature area of study.<sup>[110]</sup> Dinoop et al. studied the degradation of polystyrene by TiO<sub>2</sub>/PANI.<sup>[111]</sup> The study showed that PANI improved the light absorption of TiO<sub>2</sub> and that the efficiency of photoreduction was tuned by the PANI content until the aggregation of PANI reduced the performance. Additionally, the composites showed improved mechanical strength, thermal stability and recyclability. In a remarkable study, Sandikly et al. studied the residual toxicity of waters treated with PANI/TiO<sub>2</sub> and TiO<sub>2</sub> photocatalyst, finding that PANI/TiO<sub>2</sub> treatment exhibited a reduced toxic toward the algae cells, while astonishingly, TiO<sub>2</sub> showed a small, but not negligible, toxicity to the microorganism<sup>[112]</sup> (Figure 5a). Although the reason for the higher toxicity is still under investigation, this study provides a unique view of the electrochemical advantages of PANI and its environmental benefits. Interestingly, Fan et al. showed that AgPO<sub>4</sub>/PANI composites have important activity toward *Microcystis aeruginosa*, commonly known as a harmful algae.<sup>[113]</sup> The improved efficiency over bare AgPO<sub>4</sub> was attributed to the Z-scheme junction formed by the addition of PANI. The study suggests that the high generation of ROS could be responsible for the improved effect (Figure 5b,c). However, the selectivity of the process toward normal algae is still not clear, and the toxicity of the water after the process needs to be explored further. Despite it, ROS generation on PANI heterojunctions has been addressed in detail by Sudhir et al. who have reviewed the literature and the construction of different heterojunctions; they clearly showed that the nature of the heterojunction is still unclear, as it might be S-scheme or type-II, which could lead to different applications and solutions.<sup>[114]</sup>

Moreover, Balakumar et al. studied a ternary photocatalyst, using PANI as an anchoring and electron-transferring bridge between carbon quantum dots (CQDs) and carbon nitride (CN).<sup>[115]</sup> Their composite showed improved performance, visible light absorption, and large effectivity toward a large group of dyes and contaminants (ciprofloxacin, imidacloprid, tetracycline, phenol, and rhodamine B). Similarly, Gu et al. used CQDs and PANI as photoactive catalysts toward photo water splitting.<sup>[116]</sup> Their study showed that oxygen and hydrogen potential are reduced by 150 and 65 mV, reaching current densities of 30 and 20 mA cm<sup>-2</sup>, respectively.

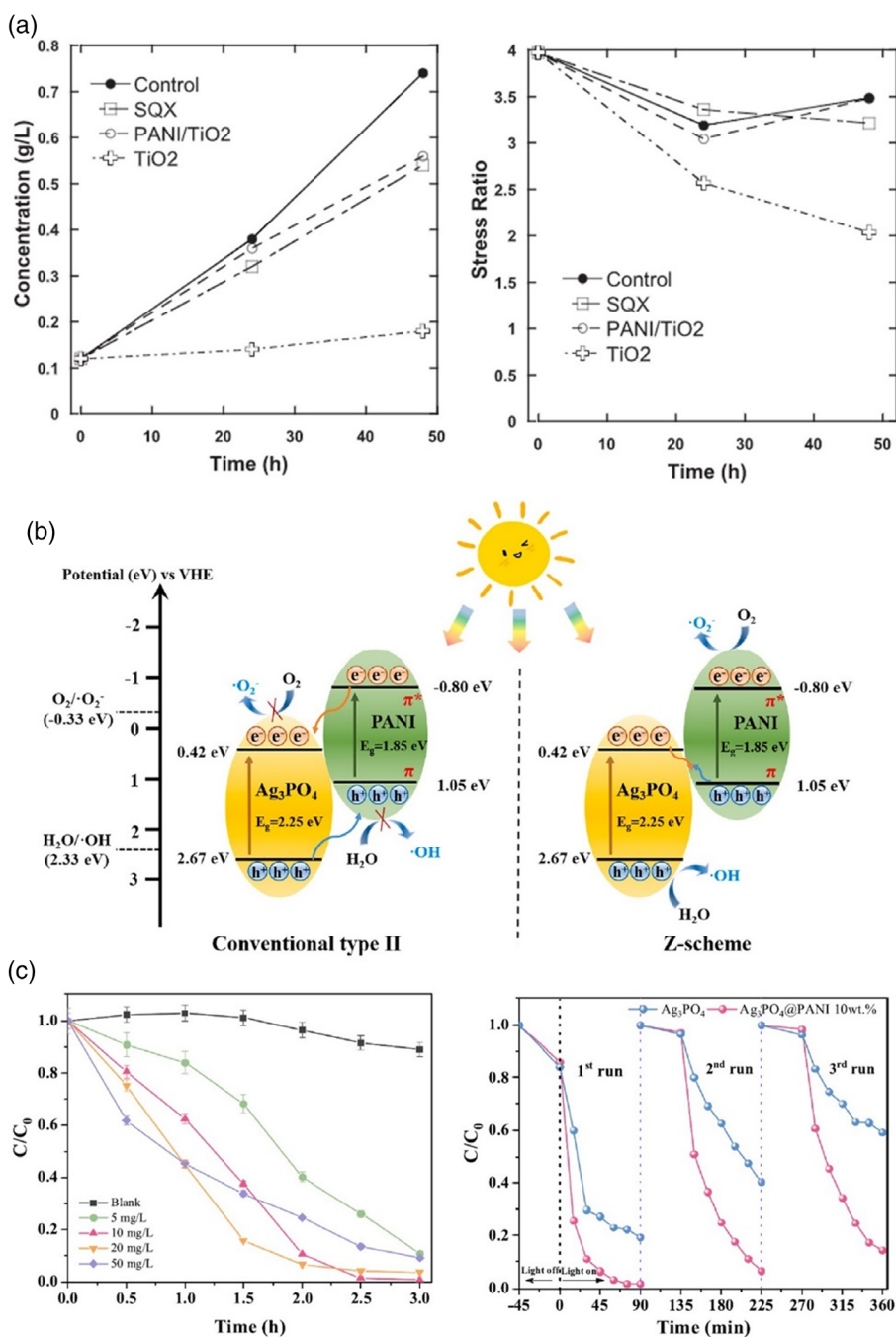


**Figure 5.** a) (Left) Variation of the biomass concentration of the microalgae *Chlorella vulgaris* versus time in the presence of the original polluted water containing 7 mg L<sup>-1</sup> of SQX ("SQX"). (Right) Variation of the stress ratio of chlorophylls for the microalgae *C. vulgaris* versus time in the presence of the original polluted water containing 7 mg L<sup>-1</sup> of SQX ("SQX"). Reproduced with permission.<sup>[112]</sup> Copyright 2021, Taylor & Francis. b) The possible photocatalytic mechanism of *M. aeruginosa* inactivation exposed to core-shell Ag<sub>3</sub>PO<sub>4</sub>@PANI 10 wt% under visible light. c) The removal efficiency of chlorophyll *a* by 10 mg L<sup>-1</sup> of under different dosages of Ag<sub>3</sub>PO<sub>4</sub>@PANI 10 wt%; (left) comparison of stability test on the MO degradation performance of Ag<sub>3</sub>PO<sub>4</sub> and Ag<sub>3</sub>PO<sub>4</sub>@PANI 10 wt% (right). Reproduced with permission.<sup>[113]</sup> Copyright 2022, Elsevier.

## 5. COFs

COFs are metal-free 2D and 3D crystalline porous polymers constructed from organic molecules through strong covalent bonds.<sup>[117,118]</sup> COFs gained increasing attention because of

their unique features, such as high crystallinity, stability under harsh conditions, large surface areas, adjustable porosity, and photocatalytic properties.<sup>[16,119,120]</sup> COFs have been widely used in electrochemistry,<sup>[121]</sup> water distillation,<sup>[122]</sup> sensing,<sup>[123]</sup> and energy.<sup>[124]</sup> The moderate bandgap (0.7–2.9 eV) energy of COFs

and bandgap engineering, which can be achieved by selecting monomers or introducing diverse functional groups, enable visible light responsive ability, making them promising materials for photocatalytic applications. Besides, COFs photocatalysts provide an enhanced photoinduced charge carriers separation and improve charge migration because of the periodic columnar  $\pi$ -arrays formed by the direct overlap of  $\pi$  orbitals between layers. However, electron transfer is often hindered, unless rational design is carried out.<sup>[125]</sup> Nevertheless, the large availability and variety of building blocks in COFs provide a promising perspective for the assembly of an efficient COF-based photocatalyst.<sup>[16]</sup>

Recently, significant progress has been made in developing COFs for photocatalytic applications, including hydrogen and oxygen evolution reactions (HER, OER), solar-driven water splitting, CO<sub>2</sub> photoreduction, photodegradation of organic pollutants, photothermal conversion, and light-induced selective oxidation.<sup>[16,119,120,126]</sup> Here, we would like to shortly overview some of the recent achievements of COFs for photocatalytic applications and then provide possible ideas for future perspectives.

As was mentioned above, COFs provide a new platform for H<sub>2</sub> photocatalytic production through HER. COFs based on acceptors like moiety, like triazine (CTFs), are considered the most promising candidates for HER due to their enhanced light absorption and efficient charge carrier separation.

However, Jang et al. developed and employed three highly crystalline imines COFs reticulated with alternating D–A (donor–acceptor) moieties of different strengths for photocatalytic HER in an ascorbic acid solution.<sup>[127]</sup> They demonstrated that developed COFs (TtaTfa) modified by the acceptor (triazine) and donor (tryphenylamine) moieties exhibit an excellent photocatalytic HER performance, reaching a remarkable HER rate of 20.7 mmol g<sup>-1</sup> h<sup>-1</sup>. They explained this excellent HER performance by the protonation of the imine linkage of these COFs, which 1) enhances the light absorption, 2) increases the charge separation efficiency, and 3) hydrophilicity. This strategy, namely, modification by acceptor and donor moieties simultaneously, demonstrates better performance than the single moiety modification (e.g., CTFs), as was previously shown by Lotsch et al. (HER rate 1.7 mmol g<sup>-1</sup> h<sup>-1</sup>)<sup>[128]</sup> and Chen et al.<sup>[129]</sup>

Efficient tuning of photocatalytic HER performance can be performed at the molecular level. Chen et al. showed that by incorporating different transition metals into the porphyrin rings of COFs, the photocatalytic hydrogen production rate of the porphyrinic (Figure 6a) COFs could be tuned.<sup>[130]</sup> Despite the HER rate having moderate values, this strategy opens new approaches for the modification of COFs photocatalysts.

Structural and compositional modification can be applied to COFs to enhance their HER performance. For instance, the

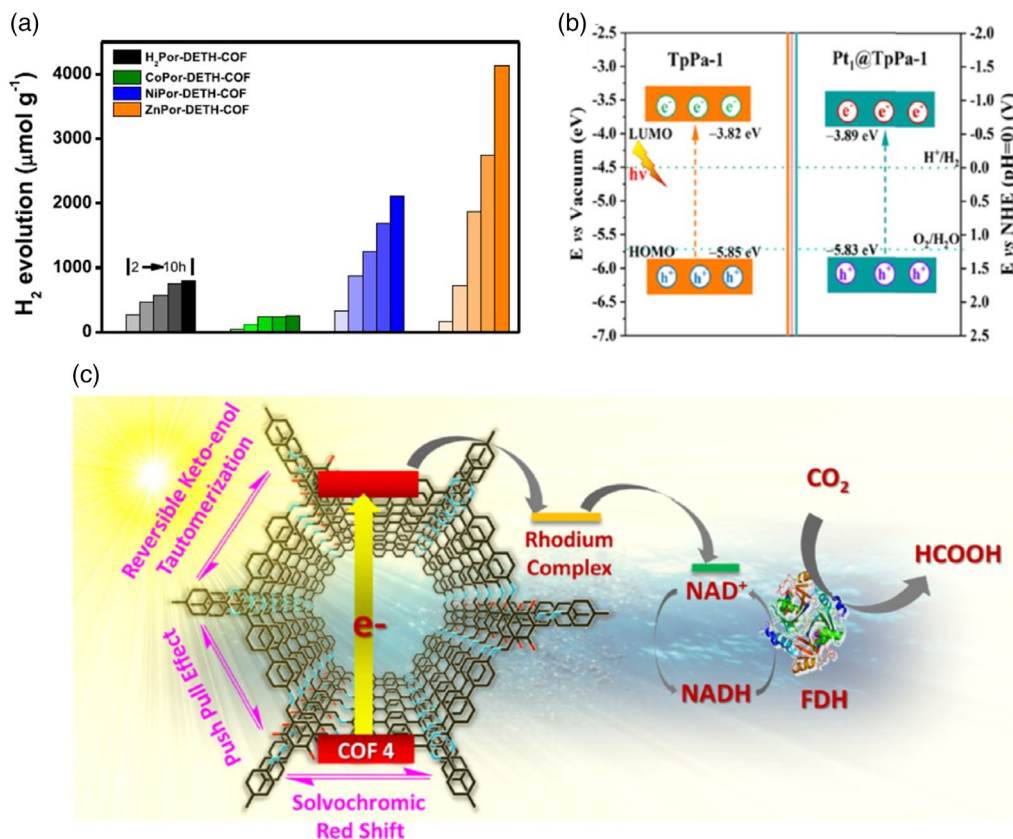


**Figure 6.** a) Time-dependent H<sub>2</sub> photogeneration using visible light for various COFs. Reproduced with permission under the terms of the Creative Commons CC BY license.<sup>[130]</sup> Copyright 2021, the Authors. Published by Springer Nature. b) Schematic energy-level diagram of TpPa-1 and Pt<sub>1</sub>@TpPa-1. Reproduced with permission.<sup>[131]</sup> Copyright 2021, American Chemical Society. c) Schematic presentation of COF photocatalyzed formic acid production. Reproduced with permission.<sup>[135]</sup> Copyright 2021, American Chemical Society.

depositions of metal nanoparticles as cocatalysts may provide a better photocatalytic performance of COFs. It was shown that single platinum atoms anchored on a COF-boosted active sites for photocatalytic HER performance<sup>[131]</sup> (Figure 6b). The developed nanocomposites based on Pt@TpPa-1 showed the photocatalytic H<sub>2</sub> evolution performance of around 100 mmol g<sup>-1</sup> h<sup>-1</sup>. The authors demonstrated that Pt single atoms reduce the energy barrier for forming H\* on the surface of COFs. This is an effective strategy for designing and developing COF-based single-atom photocatalysts with enhanced HER performance.

A combination of COFs and MOFs is another approach to improve the photocatalytic efficiency of COFs. A covalently linked NH<sub>2</sub>-MIL-68@TPA-COF nanocomposite was synthesized and was applied as the visible light-driven photocatalyst for the photodegradation of rhodamine B (RhB).<sup>[132]</sup> This nanocomposite showed an excellent photodegradation performance with a rate constant of 0.077 min<sup>-1</sup>. The authors explained this by the larger surface area and narrower bandgap.

Particular attention should be paid to 2D COFs. 2D COFs have better photocatalytic properties than bulk COF because of their planar and ordered  $\pi$ - $\pi$  stacked structures. 2D COFs are considered to be brilliant materials for various photocatalytic applications.<sup>[133,134]</sup> For instance, the electronic and photocatalytic properties of porphyrinic 2D COFs may be tuned by incorporating different transition metals into the porphyrin rings, and these COFs showed adjustable photocatalytic HER performance.<sup>[130]</sup> Chen et al. synthesized highly crystalline heptazine-based 2D COFs. They demonstrated that 2D COFs exhibited better photocatalytic activity than their bulk version because of the highly efficient separation and migration of photogenerated electron-hole pairs and efficient production of reactive oxygen species.<sup>[129]</sup> An interesting approach was applied by Singh et al. for the development of novel COFs.<sup>[135]</sup> They demonstrated that the bandgap and optical properties of keto-enol tautomerism in imine COFs could be tuned by the number of hydroxyl groups on their surfaces. These COFs were applied for visible light-induced solar fuel production utilizing abandoned carbon dioxide, and they demonstrated significantly enhanced solar light-driven 1,4-NADH regeneration up to 94.6% in 90 min to lead the formic acid production to 226.3  $\mu$ mol in 90 min (Figure 6c).

It is worth noting that the development of COFs photocatalysts is in the early stage. Compared to inorganic semiconductors, the photocatalytic efficiency of COFs is still significantly lower. However, it can be expected that COFs will find a broad application for photocatalytic HER, OER, and CO<sub>2</sub> reduction in the coming years. We may assume that preparing novel COFs modified by D-A moieties remains the main strategy to boost photocatalytic performance. This approach may improve the light absorbance and enhance the charge separation, which is critically important for photocatalysis. Besides, the creation of heterojunctions based on COFs with different 2D materials (e.g., g-C<sub>3</sub>N<sub>4</sub>, MXene, etc.) can be another approach to increase the efficiency of photocatalytic performance due to the better charge transport of photoinduced carriers. In addition to the "D-A moieties" approach, the existence of (photo)active sites, like single atom metals, metal oxides, 2D materials (e.g., MXene, black phosphorous), may also boost the photocatalytic efficiency of developed nanocomposites. Additionally, we also consider that porous fused aromatic networks (P-FANs), as part of the COF-like

materials, could play a more significant role in photocatalysis, especially if their synthetic pathways are simplified.<sup>[136]</sup>

## 6. Other Conductive Polymers

Although we have focused mainly on CS, PANI, COF, and PDA, other conductive polymers have shown some promising results. Recently, Yang et al. have prepared a hybrid material of PPy and reduced graphene oxide (RGO) to tackle both water evaporation and photocatalytic decontamination.<sup>[137]</sup> Their study shows that PPy avoids the agglomeration of RGO and allows a more efficient 3D structure. The large porosity and photoactivity of the composite provided a phenol removal of 94% and solar water evaporation of 2.08 kg m<sup>-2</sup> h<sup>-1</sup>. A recent review on this topic has been published by Kumar et al. where they compiled the recent literature on PPy composite photocatalysts, including several strategies and current developments.<sup>[138]</sup>

Nayak et al. have recently studied poly(3,4-ethylenedioxythiophene) (PEDOT) and its efficiency toward ORR. They showed that PEDOT primarily produces H<sub>2</sub>O<sub>2</sub>.<sup>[139]</sup> They studied different compositions, showing that when doping was higher, the production of H<sub>2</sub>O<sub>2</sub> increased, suggesting that biological and sensor applications might be affected by strong ORR and associated currents. Recently, Zhang et al. showed the photoelectrocatalytic reaction of PEDOT(anode) and Zis-PEDOT(cathode), focusing on the Z-scheme heterojunctions and carrier densities. They also concluded that the ZIS-PEDOT||PEDOT system could be used to enhance radical  $\cdot$ O<sup>2-</sup> and  $\cdot$ O<sup>2</sup> and further improve photoelectrocatalytic performance.

## 7. Conclusion and Perspectives

In this perspective, we report first the use of ML in designing and understanding polymeric hybrid systems toward catalytic and photocatalytic applications following describing of four types of organic-inorganic hybrid materials used as photocatalysts and based on CS, PDA, PANI, and COFs.

Although the wide development in the field of organic-inorganic hybrid materials for photocatalysis, there are still many bottlenecks to tackle to bring these materials to the market. The stability issue needs to be investigated more in all the presented materials, especially under oxidizing (in operando) conditions. The real cause of this stability should be explored, and new hybrid materials should be designed to obtain a new generation of highly stable and multifunctional photocatalytic materials. In this sense, it is imperative to include and explore the unique capabilities of the SRSPV technique, not only for well-established semiconductor surfaces but also for 2D and 2D-like COF and PDA surfaces and composites. These studies could bring a unique understanding of spatial constraints on 3D and tailored COFs.

Furthermore, here we enumerate some of the critical aspects of the future aspects that will most likely populate the literature focusing on these materials: 1) The large-scale and low-cost synthesis approaches need to be developed. Optimizing different experiment parameters is required to facilitate the production and processibility of these new materials at a commercial scale, targeting potential applicability in the large photoactive

surfaces of solar panels. 2) More extensive integrations and ex situ transferring mechanisms are required to apply in temperature, solvent, and humidity-sensitive applications, especially in PDA-based composites. 3) PDA-based nanocatalysts are expected to play a significant role in the following years. However, it is imperative to move toward standardization and control of their physical properties for broad applicability, mainly aiming at any possible market and industrial application. 4) The selectivity of the photocatalysts reaction is mainly modulated by altering the physical properties of the photocatalyst materials. There is no universal formula for selectivity, and the most accepted compromise contemplates the selective generation of ROS, which sometimes corrodes the polymeric coatings. We expect selective ROS generation to be addressed more actively in the future, as in the case of PDA/ZnO, but addressing other composites and polymers mentioned here. 5) The nature of the heterojunctions between conductive polymers and semiconductors is still debated and requires clarification. The possibility of exploiting the Z-scheme over the S-scheme would allow a whole new set of experiments, hybrid materials, and architectures toward enhanced photocatalytic performance. 6) The combination of 2D transition metal carbides and nitrides (MXenes) with the materials mentioned above may be one of the effective strategies for enhancing their photocatalytic performance due to the better charge transport of photoinduced carriers. Besides the “D–A moieties” approach, the existence of (photo)active sites, like single-atom metals and metal oxides, may also boost the photocatalytic efficiency of developed nanocomposites. 7) The integration of the polymers here reviewed with van der Waals Materials, so the heterojunctions do not crumple the 2D structure, remains challenging. Despite this, the above-reviewed studies show a general interest in combining sulfides and other families, such as tellurides and selenides. 8) Polymer may inhibit material transfer, especially for large-molecule reactants (e.g., biomass and plastics), though they can promote the transfer of carriers. This could be solved by the partial coating of inorganic semiconductors or by tuning the porosity and pore size of the coated polymer (i.e., create open pores with size larger than the molecule reactant). 9) The postcontamination of waters treated with hybrid composites is a fascinating but worrisome perspective, especially in the case shown for PANI, but it could be extrapolated to other materials. Perhaps, in this scenario, the strong resistance of PANI, which tends to limit its biodegradation, might be an advantage for the field. The mechanism and possible implications for environmental fields must be studied and extended to other conductive polymers and semiconducting catalysts. 10) SRSPV will play an essential role in studying hybrid materials toward catalysis. The study of electron transferring and the spatial distribution of electrons/holes will most definitely bring much insight into the rational design of hybrid catalysts. Especially in the case of crystalline 2D COFs and PDA/semiconductors, many important fundamental questions remain.

New concepts need to be developed to increase the lifetime of photogenerated electron/hole and enhance their generation to improve the photocatalytic efficiency of these materials for broader applications. We would also like to mention another group of materials with considerable potential for tailoring and with large available building blocks. Due to their tunable

electronic properties, variety of conjugation, and stability, conjugated polymers have already shown significant applicability toward visible light water splitting. Zhao et al. compiled a comprehensive review on the matter, providing a complete overview on the origin and methods of this fascinating field.<sup>[140]</sup>

In summary, photocatalytic water splitting based on hybrid (polymers/semiconductors) has demonstrated its promising potential for converting solar energy into clean water and molecular hydrogen. The approaches employed here could be further enhanced by tuning morphologies, coupling several inorganic and organic materials, and doping with a single atom or plasmonic materials. Given the recent literature, the outstanding results, and the prospects of these polymers, more innovative solutions are expected to address the more than ever-critical energy and environmental challenges we must definitely face in the next few decades.

## Acknowledgements

E.C. acknowledges the financial support from the National Science Centre of Poland (NCN) by the OPUS grant 2019/35/B/ST5/00248. I.I. acknowledges the financial support from the National Science Centre of Poland (NCN) by the SONATA-Bis grant 2020/38/B/ST5/00176.

## Conflict of Interest

The authors declare no conflict of interest.

## Keywords

conductive polymers, dye degradation, environmental remediation, nanocatalysts, semiconductors

Received: November 30, 2022  
Revised: December 14, 2022  
Published online: January 29, 2023

- [1] W. Zhao, M. Adeel, P. Zhang, P. Zhou, L. Huang, Y. Zhao, M. A. Ahmad, N. Shakoor, B. Lou, Y. Jiang, I. Lynch, Y. Rui, *Environ. Sci. Nano* **2022**, *9*, 61.
- [2] X. Yang, D. Wang, *ACS Appl. Energy Mater.* **2018**, *1*, 6657.
- [3] Q. Lei, S. Yang, D. Ding, J. Tan, J. Liu, R. Chen, *J. Mater. Chem. A* **2021**, *9*, 2491.
- [4] S. Zhang, L. Zhang, S. Fang, J. Zhou, J. Fan, K. Lv, *Environ. Res.* **2021**, *199*, 111259.
- [5] A. Rahman, M. M. Khan, *New J. Chem.* **2021**, *45*, 19622.
- [6] F. J. Callens, *Nukleonika* **1997**, *42*, 565.
- [7] H. Bai, S. H. Lam, J. Yang, X. Cheng, S. Li, R. Jiang, L. Shao, J. Wang, *Adv. Mater.* **2022**, *34*, 2104226.
- [8] E. Coy, K. Siuzdak, M. Pavlenko, K. Załęski, O. Graniel, M. Ziótek, S. Balme, P. Miele, M. Weber, M. Bechelany, I. Iatsunskiy, *Chem. Eng. J.* **2020**, *392*, 123702.
- [9] X.-C. Ma, Y. Dai, L. Yu, B.-B. Huang, *Light Sci. Appl.* **2016**, *5*, e16017.
- [10] X. Zhang, Y. L. Chen, R.-S. Liu, D. P. Tsai, *Rep. Prog. Phys.* **2013**, *76*, 046401.
- [11] M. Liras, M. Barawi, V. A. de la Peña O’Shea, *Chem. Soc. Rev.* **2019**, *48*, 5454.
- [12] M. Shahadat, A. Jha, Shahid-ul-Islam, R. Adnan, S. W. Ali, I. M. I. Ismail, M. Oves, S. Z. Ahammad, *Polymer* **2022**, *254*, 124975.

- [13] R. Mrówczyński, R. Markiewicz, J. Liebscher, *Polym. Int.* **2016**, 65, 1288.
- [14] H. S. Sasmal, A. Kumar Mahato, P. Majumder, R. Banerjee, *J. Am. Chem. Soc.* **2022**, 144, 11482.
- [15] E. A. Gendy, J. Iftikhar, J. Ali, D. T. Oyekunle, Z. Elkhelifa, I. I. Shahib, A. I. Khodair, Z. Chen, *J. Environ. Chem. Eng.* **2021**, 9, 105687.
- [16] C. Xia, K. O. Kirlikovali, T. H. C. Nguyen, X. C. Nguyen, Q. B. Tran, M. K. Duong, M. T. Nguyen Dinh, D. L. T. Nguyen, P. Singh, P. Raizada, V.-H. Nguyen, S. Y. Kim, L. Singh, C. C. Nguyen, M. Shokouhimehr, Q. Van Le, *Coord. Chem. Rev.* **2021**, 446, 214117.
- [17] H. Lin, C. Chen, T. Zhou, J. Zhang, *Sol. RRL* **2021**, 5, 2000458.
- [18] J. Westermayr, M. Gastegger, K. T. Schütt, R. J. Maurer, *J. Chem. Phys.* **2021**, 154, 230903.
- [19] Y. Juan, Y. Dai, Y. Yang, J. Zhang, *J. Mater. Sci. Technol.* **2021**, 79, 178.
- [20] C. Gao, X. Min, M. Fang, T. Tao, X. Zheng, Y. Liu, X. Wu, Z. Huang, *Adv. Funct. Mater.* **2022**, 32, 2108044.
- [21] M. M. Cencer, J. S. Moore, R. S. Assary, *Polym. Int.* **2022**, 71, 537.
- [22] A. Mahmood, A. Irfan, J.-L. Wang, *J. Mater. Chem. A* **2022**, 10, 4170.
- [23] A. Mahmood, J.-L. Wang, *Energy Environ. Sci.* **2021**, 14, 90.
- [24] E. C. Gok, M. O. Yildirim, M. P. U. Haris, E. Eren, M. Pegu, N. H. Hemasiri, P. Huang, S. Kazim, A. Uygun Oksuz, S. Ahmad, *Sol. RRL* **2022**, 6, 2100927.
- [25] Y. Liu, W. Yan, S. Han, H. Zhu, Y. Tu, L. Guan, X. Tan, *Sol. RRL* **2022**, 6, 2101100.
- [26] D. M. Anstine, D. S. Sholl, J. I. Siepmann, R. Q. Snurr, A. Aspuru-Guzik, C. M. Colina, *Curr. Opin. Chem. Eng.* **2022**, 36, 100795.
- [27] R. Ma, H. Zhang, T. Luo, *ACS Appl. Mater. Interfaces* **2022**, 14, 15587.
- [28] W. Zhang, W. Huang, J. Tan, Q. Guo, B. Wu, *Chemosphere* **2022**, 308, 136447.
- [29] C. Lu, Z. Xu, B. Dong, Y. Zhang, M. Wang, Y. Zeng, C. Zhang, *Carbohydr. Polym.* **2022**, 285, 119240.
- [30] T. Zhang, C. Wu, Z. Xing, J. Zhang, S. Wang, X. Feng, J. Zhu, X. Lu, L. Mu, *Mater. Today Sustainability* **2022**, 20, 100256.
- [31] Y. Xu, C.-W. Ju, B. Li, Q.-S. Ma, Z. Chen, L. Zhang, J. Chen, *ACS Appl. Mater. Interfaces* **2021**, 13, 34033.
- [32] W. Melitz, J. Shen, A. C. Kummel, S. Lee, *Surf. Sci. Rep.* **2011**, 66, 1.
- [33] J. Zhu, F. Fan, R. Chen, H. An, Z. Feng, C. Li, *Angew. Chem. Int. Ed.* **2015**, 54, 9111.
- [34] S. Wang, G. Liu, L. Wang, *Chem. Rev.* **2019**, 119, 5192.
- [35] Y. Gao, J. Zhu, H. An, P. Yan, B. Huang, R. Chen, F. Fan, C. Li, *J. Phys. Chem. Lett.* **2017**, 8, 1419.
- [36] R. Chen, Z. Ren, Y. Liang, G. Zhang, T. Dittrich, R. Liu, Y. Liu, Y. Zhao, S. Pang, H. An, C. Ni, P. Zhou, K. Han, F. Fan, C. Li, *Nature* **2022**, 610, 296.
- [37] J. Zhu, S. Pang, T. Dittrich, Y. Gao, W. Nie, J. Cui, R. Chen, H. An, F. Fan, C. Li, *Nano Lett.* **2017**, 17, 6735.
- [38] R. Chen, F. Fan, T. Dittrich, C. Li, *Chem. Soc. Rev.* **2018**, 47, 8238.
- [39] R. Chen, F. Fan, C. Li, *Angew. Chem. Int. Ed.* **2022**, 61, <https://doi.org/10.1002/anie.202117567>.
- [40] X. Wan, Y. Gao, M. Eshete, M. Hu, R. Pan, H. Wang, L. Liu, J. Liu, J. Jiang, S. Brovelli, J. Zhang, *Nano Energy* **2022**, 98, 107217.
- [41] V. Aubriet, K. Courouble, O. Bardagot, R. Demadrille, Ł. Borowik, B. Grévin, *Nanotechnology* **2022**, 33, 225401.
- [42] L. Meyer-Déru, G. David, R. Auvergne, *Carbohydr. Polym.* **2022**, 295, 119877.
- [43] S. Peers, A. Montembault, C. Ladavière, *Carbohydr. Polym.* **2022**, 275, 118689.
- [44] Y. Yue, K. Hou, J. Chen, W. Cheng, Q. Wu, J. Han, J. Jiang, *ACS Appl. Mater. Interfaces* **2022**, 14, 24708.
- [45] K. T. Karthikeyan, A. Nithya, K. Jothivenkatachalam, *Int. J. Biol. Macromol.* **2017**, 104, 1762.
- [46] T. Kamal, M. Ul-Islam, S. B. Khan, A. M. Asiri, *Int. J. Biol. Macromol.* **2015**, 81, 584.
- [47] G. Madhan, A. A. Begam, L. V. Varsha, R. Ranjithkumar, D. Bharathi, *Int. J. Biol. Macromol.* **2021**, 190, 259.
- [48] H. Zhu, R. Jiang, L. Xiao, Y. Chang, Y. Guan, X. Li, G. Zeng, *J. Hazard. Mater.* **2009**, 169, 933.
- [49] H. Shen, D. P. Durkin, A. Aiello, T. Diba, J. Lafleur, J. M. Zara, Y. Shen, D. Shuai, *J. Hazard. Mater.* **2021**, 408, 124890.
- [50] S. Zhang, Saeeda, A. Khan, N. Ali, S. Malik, H. Khan, N. Ali, H. M. N. Iqbal, M. Bilal, *Environ. Res.* **2022**, 213, 113722.
- [51] P. Sirajudheen, V. C. Resha Kasim, C. P. Nabeena, M. C. Basheer, S. Meenakshi, *Mater. Today Proc.* **2021**, 47, 2553.
- [52] B. Janani, M. K. Okla, M. A. Abdel-Maksoud, H. Abdelgawad, A. M. Thomas, L. L. Raju, W. H. Al-Qahtani, S. S. Khan, *J. Environ. Manage.* **2022**, 306, 114396.
- [53] Y. Liu, W. Shen, Q. Li, J. Shu, L. Gao, M. Ma, W. Wang, H. Cui, *Nat. Commun.* **2017**, 8, 1003.
- [54] Y. Li, J. Ma, D. Jin, G. Jiao, X. Yang, K. Liu, J. Zhou, R. Sun, *Appl. Catal., B* **2021**, 291, 120123.
- [55] B. Zhang, F. Liu, C. Nie, Y. Hou, M. Tong, *J. Hazard. Mater.* **2022**, 435, 128966.
- [56] S. Panda, K. Deshmukh, S. K. Khadheer Pasha, J. Theerthagiri, S. Manickam, M. Y. Choi, *Coord. Chem. Rev.* **2022**, 462, 214518.
- [57] V. Myndrul, E. Coy, N. Babayevska, V. Zahorodna, V. Balitskiy, I. Baginskiy, O. Gogotsi, M. Bechelany, M. T. Giardi, I. Iatsunskiy, *Biosens. Bioelectron.* **2022**, 207, 114141.
- [58] Y. Tang, C. Yang, X. Xu, Y. Kang, J. Henzie, W. Que, Y. Yamauchi, *Adv. Energy Mater.* **2022**, 12, 2103867.
- [59] Y. Wang, B. Jiang, T. Sun, S. Wang, Y. Jin, *J. Mater. Chem. C* **2022**, 10, 8043.
- [60] Z. Tan, H. Zhao, F. Sun, L. Ran, L. Yi, L. Zhao, J. Wu, *Composites, Part A* **2022**, 155, 106809.
- [61] G. Yang, X. Hu, J. Liang, Q. Huang, J. Dou, J. Tian, F. Deng, M. Liu, X. Zhang, Y. Wei, *J. Hazard. Mater.* **2021**, 419, 126220.
- [62] L. Wang, D. Wang, K. Wang, K. Jiang, G. Shen, *ACS Mater. Lett.* **2021**, 3, 921.
- [63] H. Feinberg, T. W. Hanks, *Polym. Int.* **2022**, 71, 578.
- [64] S. Sakib, F. Bakhshandeh, S. Saha, L. Soleymani, I. Zhitomirsky, *Sol. RRL* **2021**, 5, 2100512.
- [65] H. Musarurwa, N. Tawanda Tavengwa, *Chemosphere* **2021**, 266, 129222.
- [66] M. L. Alfieri, T. Weil, D. Y. W. Ng, V. Ball, *Adv. Colloid Interface Sci.* **2022**, 305, 102689.
- [67] H. Lee, S. M. Dellatore, W. M. Miller, P. B. Messersmith, *Science* **2007**, 318, 426.
- [68] J. H. Ryu, P. B. Messersmith, H. Lee, *ACS Appl. Mater. Interfaces* **2018**, 10, 7523.
- [69] J. Liebscher, R. Mrówczyński, H. A. Scheidt, C. Filip, N. D. Hädade, R. Turcu, A. Bende, S. Beck, *Langmuir* **2013**, 29, 10539.
- [70] P. Samyn, *Int. J. Biol. Macromol.* **2021**, 178, 71.
- [71] F. Ponzio, P. Payamyar, A. Schneider, M. Winterhalter, J. Bour, F. Addiego, M.-P. Krafft, J. Hemmerle, V. Ball, *J. Phys. Chem. Lett.* **2014**, 5, 3436.
- [72] J. Szewczyk, D. Aguilar-Ferrer, E. Coy, *Eur. Polym. J.* **2022**, 174, 111346.
- [73] F. Chen, Y. Xing, Z. Wang, X. Zheng, J. Zhang, K. Cai, *Langmuir* **2016**, 32, 12119.
- [74] D. Aguilar-Ferrer, J. Szewczyk, E. Coy, *Catal. Today* **2022**, 397–399, 316.
- [75] K. Tadzyszak, R. Mrówczyński, R. Carmieli, *J. Phys. Chem. B* **2021**, 125, 841.
- [76] E. Coy, I. Iatsunskiy, J. C. Colmenares, Y. Kim, R. Mrówczyński, *ACS Appl. Mater. Interfaces* **2021**, 13, 23113.
- [77] T. Marchesi D'Alvise, S. Harvey, L. Hueske, J. Szelwicka, L. Veith, T. P. J. Knowles, D. Kubiczek, C. Flaig, F. Port, K. Gottschalk,

- F. Rosenau, B. Graczykowski, G. Fytas, F. S. Ruggeri, K. Wunderlich, T. Weil, *Adv. Funct. Mater.* **2020**, *30*, 2000378.
- [78] S. A. Pawar, A. N. Chand, A. V. Kumar, *ACS Sustainable Chem. Eng.* **2019**, *7*, 8274.
- [79] R. Mrówczyński, A. Bunge, J. Liebscher, *Chem. - A Eur. J.* **2014**, *20*, 8647.
- [80] Q. Huang, J. Chen, M. Liu, H. Huang, X. Zhang, Y. Wei, *Chem. - Eur. J.* **2020**, *387*, 124019.
- [81] V. Fedorenko, D. Damberga, K. Grundsteins, A. Ramanavicius, S. Ramanavicius, E. Coy, I. Iatsunskiy, R. Viter, *Polymers* **2021**, *13*, 2918.
- [82] D. Damberga, V. Fedorenko, K. Grundsteins, Ş. Altundal, A. Šutka, A. Ramanavicius, E. Coy, R. Mrówczyński, I. Iatsunskiy, R. Viter, *Nanomaterials* **2020**, *10*, 2438.
- [83] V. Fedorenko, R. Viter, R. Mrówczyński, D. Damberga, E. Coy, I. Iatsunskiy, *RSC Adv.* **2020**, *10*, 29751.
- [84] N. Nie, F. He, L. Zhang, B. Cheng, *Appl. Surf. Sci.* **2018**, *457*, 1096.
- [85] G. Han, F. Xu, B. Cheng, Y. Li, J. Yu, L. Zhang, *Acta Phys. Chim. Sin.* **2022**, *38*, 2112037.
- [86] X. Zhang, J. Yu, W. Macyk, S. Wageh, A. A. Al-Ghamdi, L. Wang, *Adv. Sustainable Syst.* **2022**, 2200113, <https://doi.org/10.1002/advs.202200113>.
- [87] L. Wang, J. Zhang, H. Yu, I. H. Patir, Y. Li, S. Wageh, A. A. Al-Ghamdi, J. Yu, *J. Phys. Chem. Lett.* **2022**, *13*, 4695.
- [88] Y. Kim, E. Coy, H. H. J. H. Kim, R. Mrówczyński, P. Torruella, D.-W. Jeong, K. S. Choi, J. H. Jang, M. Y. Song, D.-J. Jang, F. Peiro, S. Jurga, H. H. J. H. Kim, *Appl. Catal., B* **2021**, *280*, 119423.
- [89] W. Wang, M. Li, X. Huang, J. Fang, F. Peng, H. Huang, *Appl. Surf. Sci.* **2022**, *601*, 154114.
- [90] X. Liu, T. Zhang, Y. Li, J. Zhang, Y. Du, Y. Yang, Y. Jiang, K. Lin, *Chem. Eng. J.* **2022**, *434*, 134602.
- [91] J. Lu, C. Fang, G. Wang, L. Zhu, *Ind. Eng. Chem. Res.* **2022**, *61*, 1100.
- [92] Z. Wei, S. Zhao, W. Li, X. Zhao, C. Chen, D. L. Phillips, Y. Zhu, W. Choi, *ACS Catal.* **2022**, *12*, 11436.
- [93] S. S. Ruppel, J. Liang, *Langmuir* **2022**, *38*, 5020.
- [94] M. Alfieri, L. Panzella, S. Oscurato, M. Salvatore, R. Avolio, M. Errico, P. Maddalena, A. Napolitano, M. D'Ischia, *Biomimetics* **2018**, *3*, 26.
- [95] J. Szewczyk, M. Pochylski, K. Szutkowski, M. Kempirski, R. Mrówczyński, I. Iatsunskiy, J. Gapiński, E. Coy, *Mater. Today Chem.* **2022**, *24*, 100935.
- [96] A. Olejnik, M. Ficek, K. Siuzdak, R. Bogdanowicz, *Electrochim. Acta* **2022**, *409*, 140000.
- [97] A. Olejnik, M. Ficek, M. Szkodo, A. Stanisławska, J. Karczewski, J. Ryl, A. Dołęga, K. Siuzdak, R. Bogdanowicz, *ACS Nano* **2022**, *16*, 13183.
- [98] M. D. Nothling, C. G. Bailey, L. L. Fillbrook, G. Wang, Y. Gao, D. R. McCamey, M. Monfared, S. Wong, J. E. Beves, M. H. Stenzel, *J. Am. Chem. Soc.* **2022**, *144*, 6992.
- [99] T. Vasileiadis, T. Marchesi D'Alvise, C.-M. Saak, M. Pochylski, S. Harvey, C. V. Synatschke, J. Gapinski, G. Fytas, E. H. G. Backus, T. Weil, B. Graczykowski, *Nano Lett.* **2021**, *22*, 578.
- [100] A. Samadi, M. Xie, J. Li, H. Shon, C. Zheng, S. Zhao, *Chem. Eng. J.* **2021**, *418*, 129425.
- [101] H. N. Heme, M. S. N. Alif, S. M. S. M. Rahat, S. B. Shuchi, *J. Energy Storage* **2021**, *42*, 103018.
- [102] M. Beygisangchin, S. Abdul Rashid, S. Shafie, A. R. Sadrolhosseini, H. N. Lim, *Polymers* **2021**, *13*, 2003.
- [103] V. Babel, B. L. Hiran, *Polym. Compos.* **2021**, *42*, 3142.
- [104] C. Bavatharani, E. Muthusankar, S. M. Wabaidur, Z. A. Alothman, K. M. Alsheetan, M. mana AL-Anazy, D. Ragupathy, *Synth. Met.* **2021**, *271*, 116609.
- [105] B. Fang, J. Yan, D. Chang, J. Piao, K. M. Ma, Q. Gu, P. Gao, Y. Chai, X. Tao, *Nat. Commun.* **2022**, *13*, 2101.
- [106] S. Senguttuvan, P. Senthilkumar, V. Janaki, S. Kamala-Kannan, *Chemosphere* **2021**, *267*, 129201.
- [107] F. Zhang, Y. Zhang, G. Zhang, Z. Yang, D. D. Dionysiou, A. Zhu, *Appl. Catal., B* **2018**, *236*, 53.
- [108] F. Zhang, Y. Zhang, Y. Wang, A. Zhu, Y. Zhang, *Sep. Purif. Technol.* **2022**, *283*, 120161.
- [109] M. Faisal, F. A. Harraz, A. A. Ismail, M. A. Alsaiani, S. A. Al-Sayari, M. S. Al-Assiri, *Ceram. Int.* **2019**, *45*, 20484.
- [110] N. K. Jangid, S. Jadoun, A. Yadav, M. Srivastava, N. Kaur, *Polym. Bull.* **2021**, *78*, 4743.
- [111] S. Dinooplal, T. Sunil Jose, C. Rajesh, P. Anju Rose Puthukkara, K. Savitha Unnikrishnan, K. J. Arun, *Eur. Polym. J.* **2021**, *153*, 110493.
- [112] N. Sandikly, M. Kassir, M. El Jamal, H. Takache, P. Arnoux, S. Mokh, M. Al-Iskandarani, T. Roques-Carmes, *Environ. Technol.* **2021**, *42*, 419.
- [113] G. Fan, X. Li, X. Chen, Y. You, W. Dai, F. Qu, D. Tang, Z. Yan, *Chem. Eng. J.* **2022**, *427*, 132005.
- [114] O. S. Ekande, M. Kumar, *J. Environ. Chem. Eng.* **2021**, *9*, 105725.
- [115] V. Balakumar, M. Ramalingam, K. Sekar, C. Chuaicham, K. Sasaki, *Chem. Eng. J.* **2021**, *426*, 131739.
- [116] X. Gu, Z. Chen, Y. Li, J. Wu, X. Wang, H. Huang, Y. Liu, B. Dong, M. Shao, Z. Kang, *ACS Appl. Mater. Interfaces* **2021**, *13*, 24814.
- [117] Y. Zeng, R. Zou, Z. Luo, H. Zhang, X. Yao, X. Ma, R. Zou, Y. Zhao, *J. Am. Chem. Soc.* **2015**, *137*, 1020.
- [118] C. S. Diercks, O. M. Yaghi, *Science*, **2017**, *355*, 923.
- [119] J. You, Y. Zhao, L. Wang, W. Bao, *J. Clean. Prod.* **2021**, *291*, 125822.
- [120] H. Li, L. Wang, G. Yu, *Nano Today* **2021**, *40*, 101247.
- [121] X. Zhao, P. Pachfule, A. Thomas, *Chem. Soc. Rev.* **2021**, *50*, 6871.
- [122] S. Zhao, C. Jiang, J. Fan, S. Hong, P. Mei, R. Yao, Y. Liu, S. Zhang, H. Li, H. Zhang, C. Sun, Z. Guo, P. Shao, Y. Zhu, J. Zhang, L. Guo, Y. Ma, J. Zhang, X. Feng, F. Wang, H. Wu, B. Wang, *Nat. Mater.* **2021**, *20*, 1551.
- [123] Z. Meng, K. A. Mirica, *Chem. Soc. Rev.* **2021**, *50*, 13498.
- [124] W. Wang, V. S. Kale, Z. Cao, Y. Lei, S. Kandambeth, G. Zou, Y. Zhu, E. Abouhamad, O. Shekhal, L. Cavallo, M. Eddaoudi, H. N. Alshareef, *Adv. Mater.* **2021**, *33*, 2103617.
- [125] W. Qiu, Y. He, L. Li, Z. Liu, S. Zhong, Y. Yu, *Langmuir* **2021**, *37*, 11535.
- [126] Z. Chen, Y. Su, X. Tang, X. Zhang, C. Duan, F. Huang, Y. Li, *Sol. RRL* **2021**, *5*, 2100762.
- [127] J. Yang, A. Acharjya, M. Ye, J. Rabeah, S. Li, Z. Kochovski, S. Youk, J. Roeser, J. Grüneberg, C. Penschke, M. Schwarze, T. Wang, Y. Lu, R. Krol, M. Oschatz, R. Schomäcker, P. Saalfrank, A. Thomas, *Angew. Chem. Int. Ed.* **2021**, *60*, 19797.
- [128] V. S. Vyas, F. Haase, L. Stegbauer, G. Savasci, F. Podjaski, C. Ochsenfeld, B. V. Lotsch, *Nat. Commun.* **2015**, *6*, 8508.
- [129] D. Chen, W. Chen, G. Zhang, S. Li, W. Chen, G. Xing, L. Chen, *ACS Catal.* **2022**, *12*, 616.
- [130] R. Chen, Y. Wang, Y. Ma, A. Mal, X.-Y. Gao, L. Gao, L. Qiao, X.-B. Li, L.-Z. Wu, C. Wang, *Nat. Commun.* **2021**, *12*, 1354.
- [131] P. Dong, Y. Wang, A. Zhang, T. Cheng, X. Xi, J. Zhang, *ACS Catal.* **2021**, *11*, 13266.
- [132] Y. Peng, M. Zhao, B. Chen, Z. Zhang, Y. Huang, F. Dai, Z. Lai, X. Cui, C. Tan, H. Zhang, *Adv. Mater.* **2018**, *30*, 1705454.
- [133] X. Li, S. Yang, F. Zhang, L. Zheng, X. Lang, *Appl. Catal., B* **2022**, *303*, 120846.

- [134] H. Hao, F. Zhang, X. Dong, X. Lang, *Appl. Catal. B*, **2021**, 299, 120691.
- [135] N. Singh, D. Yadav, S. V. Mulay, J. Y. Kim, N.-J. Park, J.-O. Baeg, *ACS Appl. Mater. Interfaces* **2021**, 13, 14122.
- [136] I. Ahmad, J. Mahmood, J.-B. Baek, *Small Sci.* **2021**, 1, 2000007.
- [137] S. Yan, H. Song, Y. Li, J. Yang, X. Jia, S. Wang, X. Yang, *Appl. Catal., B* **2022**, 301, 120820.
- [138] R. Kumar, P. Raizada, T. Ahamad, S. M. Alshehri, Q. Van Le, T. S. Alomar, V.-H. Nguyen, R. Selvasembian, S. Thakur, D. C. Nguyen, P. Singh, *Chemosphere* **2022**, 303, 134993.
- [139] P. D. Nayak, D. Ohayon, S. Wustoni, S. Inal, *Adv. Mater. Technol.* **2022**, 7, 2100277.
- [140] C. Zhao, Z. Chen, R. Shi, X. Yang, T. Zhang, *Adv. Mater.* **2020**, 32, 1907296.